Theoretical and Applied Climatology (2025) 156:179
https://doi.org/10.1007/s00704-025-05405-2

RESEARCH

Current and projected changes in climate extremes and agro-climatic zones over East Africa

Teferi Demissie[1,2] · Gulilat T. Diro[3] · Confidence Duku[4] · Dawit Solomon[1] · Tamirat B. Jimma[5]

Received: 21 May 2024 / Accepted: 11 February 2025 / Published online: 27 February 2025

Abstract

Given the sensitivity of the agricultural sector to climate variability and change, a comprehensive understanding of environmental factors to this sector and the extent to which climate change may alter such factors is critical for planning and adaptation strategies. This study aims to assess the extent of extreme climate conditions and livestock-relevant maps of agro-climatic zones across East Africa in current and future climates. Ensembles of seven global climate models selected from the sixth Coupled Model Intercomparison Project (CMIP6) are considered under SSP245 and SSP585 socio-economic pathways. The water extreme/stress indicators considered include indices to indicate drought and flood situations. The heat stress indicators are composed of the frequency of hot spells and the duration and intensity of heat waves. As expected, all heat stress indicators are projected to increase in future climates. The frequency and intensity of heavy precipitation events are also projected to increase with increased GHG emissions. The drought stress indicators follow the precipitation pattern and are projected to decline over most of the domain. A heterogeneous response of the agro-climate regime to climate changes is projected for eastern Africa, with some areas (e.g., southern Tanzania) experiencing alterations towards drier zones while others (e.g., northern Somalia, South Sudan) are experiencing a shift towards wetter zones. The increase in short-duration heavy precipitation events together with the enhanced pace of heat stress over the region, will have critical implications for agriculture in general and local livestock production in particular.

1 Introduction

Climate change is a pressing global issue with significant implications for agro-climatic zones worldwide, affecting agricultural productivity, food security, and ecosystem stability. Africa is particularly vulnerable to the impacts of climate change due to its reliance on rain-fed agriculture and limited adaptive capacity. East Africa has diverse climatic conditions ranging from hot and dry conditions over the northern rift valley of the Afar region to cold and wet areas of the Ethiopian highlands and parts of Uganda and Congo. Such heterogeneity across the region arises due to the complex topography of the region, as well as due to the unique interaction of local microclimate, regional circulation, large-scale modes of variability, and the global climate system. The large-scale drivers include Inter-tropical Convergence Zone (Diro et al. 2011a), equatorial Pacific sea surface temperature (Diro et al. 2011b; Gleixner et al. 2017), Indian Ocean Dipole (Bahaga et al. 2015; Kolstad et al. 2021) and other global modes of variabilities (Segele et al. 2009a, b; Zeleke et al. 2013). The underlying heterogeneous surface impact includes effects from lakes (Anyah and Semazzi 2004; Fairman et al. 2011) and complex topography (Slingo et al. 2005). Regarding the rainfall regime, the equatorial regions have two rainy seasons, the main

✉ Teferi Demissie
t.demissie@cgiar.org

Gulilat T. Diro
gulilattef@gmail.com

Confidence Duku
confidence.duku@wur.nl

Dawit Solomon
d.solomon@cgiar.org

Tamirat B. Jimma
jimma.tamirat@aau.edu.et

1 International Livestock Research Institute (ILRI), Accelerating Impacts of CGIAR Climate Research for Africa (AICCRA), Addis Ababa, P.O. Box 5689, Ethiopia

2 Norwegian Meteorological Institute, 0313 Oslo, Norway

3 Department of Earth and Atmospheric Sciences, University of Quebec at Montreal, 201 President Kennedy Avenue, Montreal H2X 3Y7, Canada

4 Wageningen Environmental Research, P.O. Box 47, 6700AA Wageningen, The Netherlands

5 IGSSA, Addis Ababa University, King George VI, P.O.Box 1176, Addis Ababa, Ethiopia

or long rainy season from March to May and a short or secondary season from October to December. The northern part of East Africa, namely northern Ethiopia, Eritrea, and Sudan, has a single rainfall season from June to September.

The Intergovernmental Panel on Climate Change (IPCC) assessment reports and other studies have demonstrated the consequence of increased greenhouse gas (GHG) concentrations on climate, albeit on a global and regional level (Stocker et al. 2014; Sillmann et al. 2013). Furthermore, several studies have investigated future changes in the climate of East Africa under different emission scenarios (Dosio et al. 2021; Li et al. 2016; Otieno and Anyah 2013; Zhou et al. 2021). Most of these studies either focus on the evaluation of CMIP models for current climates (e.g., (Akinsanola, et al. 2021; Ayugi et al. 2021a, b), projected changes to the climate mean variables (Dosio et al. 2021), or use the previous generations of global models (Tan et al. 2020; Ongoma et al. 2018). However, less emphasis has been given to the detailed regional analysis of livestock-specific extreme climate indices both for current and future climates from the recent CMIP6 models. Therefore, one of the aims of this assessment is to enhance the understanding of the current and future extreme climate hazards and impacts of climate change, which will help feed the livestock sector's adaptation strategies. In particular, we evaluate sector-specific extreme indices over East Africa for present-day climate and projected changes for future horizons based on ensembles of seven CMIP6 global climate models and two future emission (SSP245 and SSP585) scenarios.

It is important to note that having diverse climatic conditions, as in East Africa, has resulted in different land use patterns and, hence, agricultural practices such as crop cultivation in the wet and livestock production in the semi-arid and arid regions. In most semi-arid regions, livestock production enables farmers to diversify incomes and is crucial for coping mechanisms in the poor households. Previous studies (Kruska et al. 2003; Steinfeld et al. 2006; Thornton 2010) have noted that production and demand for livestock products are increasing throughout the developing world, including Africa. Nevertheless, climate variability and change pose significant challenges for the agriculture sector in general and in livestock production systems in particular. This assessment will help us to gain a better understanding of the location of suitable environmental factors related to livestock production currently found and how anthropogenic climate change may lead to shifts in the location of these environmental factors. This, in turn, should lead to improved dissemination of intervention options. One of the specific objectives of this study is to determine the variation in agro-climatological zones over East Africa associated with anthropogenic climate change. This includes classifying the East African region into homogeneous agro-climatic zones for the historical climate period as well as comparing the future changes with respect to the current situation using ensemble mean of global climate model output from the six phases of Coupled Model Intercomparison Project (O'neill et al. 2016) under SSP245 and SSP585 emission scenarios.

2 Data, models, and methods

2.1 Observational dataset and models

For this assessment, multiple datasets containing various climate variables are considered. These include precipitation, daily maximum and minimum temperature fields from the Climate Research Unit (Harris et al. 2020) at monthly temporal resolution. CRU datasets are station datasets interpolated over land grid points at multiple spatial resolutions such as $0.5° \times 0.5°$ or $1° \times 1°$ horizontal resolutions. While the dataset spans from 1901 to the present day, analysis is carried out only for the recent 30 years covering the 1985–2014 period to match the historical model simulation. Furthermore, the daily precipitation dataset from Climate Hazards Group InfraRed Precipitation with Stations (Funk et al. 2015) and daily maximum and minimum temperature fields from the fifth generation of the European Centre for Medium-Range Weather Forecasts (ECMWF) reanalysis (Hersbach et al. 2019) are employed to derive water and heat stress indicators. CHIRPS uses TIR imagery and gauge data in addition to a monthly precipitation climatology, CHPClim, and atmospheric model rainfall fields from the NOAA Climate Forecast System, version 2 (CFSv2). ERA-5 is produced by combining the Integrated Forecast System with data assimilation at a spatial resolution of 0.25° grid and at an hourly time interval (Hersbach et al. 2019). Please note that all data are aggregated to a common horizontal grid of $1° \times 1°$ resolution.

Seven global climate models participating in the sixth phase of the coupled model intercomparison project (O'neill et al. 2016) framework were selected and retrieved from the ESGF portal. The lists of these GCMs and references are listed in Table 1. This assessment considers climate variables such as precipitation and temperature at daily frequency.

2.2 Methods

The model data obtained for assessment is on daily frequency running from 1985 until 2100. Three analysis periods are chosen: the reference or historical period (1985–2014) and the future. For future climate, two representative concentration pathways (SSP245 and SSP585) were considered (O'neill et al. 2016).

2.2.1 Extreme climate indices

Several widely used indices of heat stress, water availability, and drought risk indicators were analyzed to study the mean annual conditions in current and future climates. These extreme indices were selected from the list developed by the Expert Team on Sector-Specific Climate Indices (ET-SCI) set up by the World Meteorological Organization–Commission for Climatology (WMO–CCL). The ET-SCI indices are computed by ClimPACTv2 (Alexander and Herold 2016). While

Table 1 CMIP6 model name, horizontal resolution, and key references

Model	Resolution	Reference
CMCC	0.94° × 1.25°	(Cherchi et al. 2019)
GFDL-ESM4	1.3° × 1°	(Held et al. 2019)
EC-Earth3	0.7° × 0.7°	(Massonnet et al. 2020)
MPI-ESM1-2-HR	0.9° × 0.9°	(Gutjahr et al. 2018)
NorESM2-MM	1.25° × 0.94°	(Seland et al. 2020)
INM-CM5-0	2° × 1.5°	(Volodin et al. 2018)
MRI-ESM2-0	1.1° × 1.1°	(Yukimoto et al. 2019)

ClimPACTv2 computes over 60 ET-SCI sector-specific indices, we analyze a subset of indices relevant to the agricultural sector. The list of ET-SCI indices used in this assessment is presented in Table 2. Please note that future extreme indices are computed based on threshold values obtained from historical simulations. This implies that the projected changes are described with regard to changes in the historical climate distribution.

These hydrometeorological variables are estimated from climate model output for present-day as well as for future time horizons with two representative concentration pathways. For climate change assessment, each time horizon is set to 30 years as recommended by WMO's guide to climatological practices. Whenever current and future climate conditions are compared, a two-sided student T-test considering unequal variance at 0.05 significance level is performed to determine if the mean values are significantly different between the two climates.

2.2.2 Agro-climatological classification

The agro-climatic classification is based on the length of the growing period (LGP), which is defined as the period in days during the year when the daily precipitation amount is greater than half the potential evapotranspiration (PET). Here, the potential evapotranspiration will be represented by reference evapotranspiration, which is considered as a proxy for the water requirement under well-watered conditions. Although several methods are available for estimating ETo, Hargreaves (Hargreaves and Samani 1985) is employed due to its simplicity and the accuracy of estimates. i.e.,

$$ET_o = 0.0023\left(T_{mean} + 17.8\right)\left(T_{max} - T_{min}\right)^{0.5} R_a$$

where Tmean, Tmax, Tmin, and R_a are the mean, maximum, minimum temperatures and extraterrestrial radiation, respectively.

Following (Sere 1996; Seré et al. 1996), four agro-climatic zones- Arid (A), Semi-Arid (SA), sub-humid (SH), and Humid (H) are defined using the length of growing periods according to the following thresholds. Zone A is when the length of growing period is less than 75 days; Zone H is for regions where the length of growing period is greater than 270 days. For SA, the length of growing period is in the range of 75 and 180. The remaining zone, SH, is when the length of the growing period is in the range of 180 and 270.

3 Result and discussions

3.1 Evaluation and present-day conditions

3.1.1 Spatial pattern and annual cycle

Figures 1 and 2 show the spatial pattern of annual precipitation climatology and maximum temperature climatology from observations and all GCMs considered. The figures indicate that mean annual rainfall and temperature vary dramatically following the topography. The spatial distribution of precipitation and temperature from observation data revealed drier and warmer

Table 2 Extreme climate indices used in this assessment

Index	Indicator name	Definition	Uint
R20mm	Number of extreme heavy rainy days	No. of days for which PR > 20 mm/day	days
Prcptot	Total wet-day precipitation	Sum of daily PR > = 1 mm	mm
R95ptot	Fraction of total annual PR from heavy rainy days	100* (Annual sum of daily PR > 95th Percentile)/Prcptot	%
Rx5day	Max. 5-day PR	Max. 5-day PR total	mm
CDD	Consecutive dry days	Max. annual number of consecutive dry days (PR < 1 mm)	days
SPI	Standardized Precipitation Index	Measure of 'drought' on a scale of 3, 6, and 12 months (McKee 1995)	Unitless
SPEI	Standardized Precipitation Evaporation Index	A measure of 'drought' on scale of 3,6, and12 months (Beguería et al. 2010)	Unitless
WSDI	Warm spell duration indicator	Annual number of days contributing to events in which 6 or more consecutive days experience Tmax > 90th percentile	days
Txge35	Number of hot days	Annual number of days for which Tx is > = 35 °C	days
TXx	Annual maximum daily temperature	Annual daily maximum temperature	°C
HWD	Heat wave duration	The length of the longest duration of the heat wave	Days
HWA	Heatwave amplitude	The peak daily Tmax value in the hottest heat wave	°C
HWM	Heatwave magnitude	The mean temperature of all heat waves identified by HWN	°C

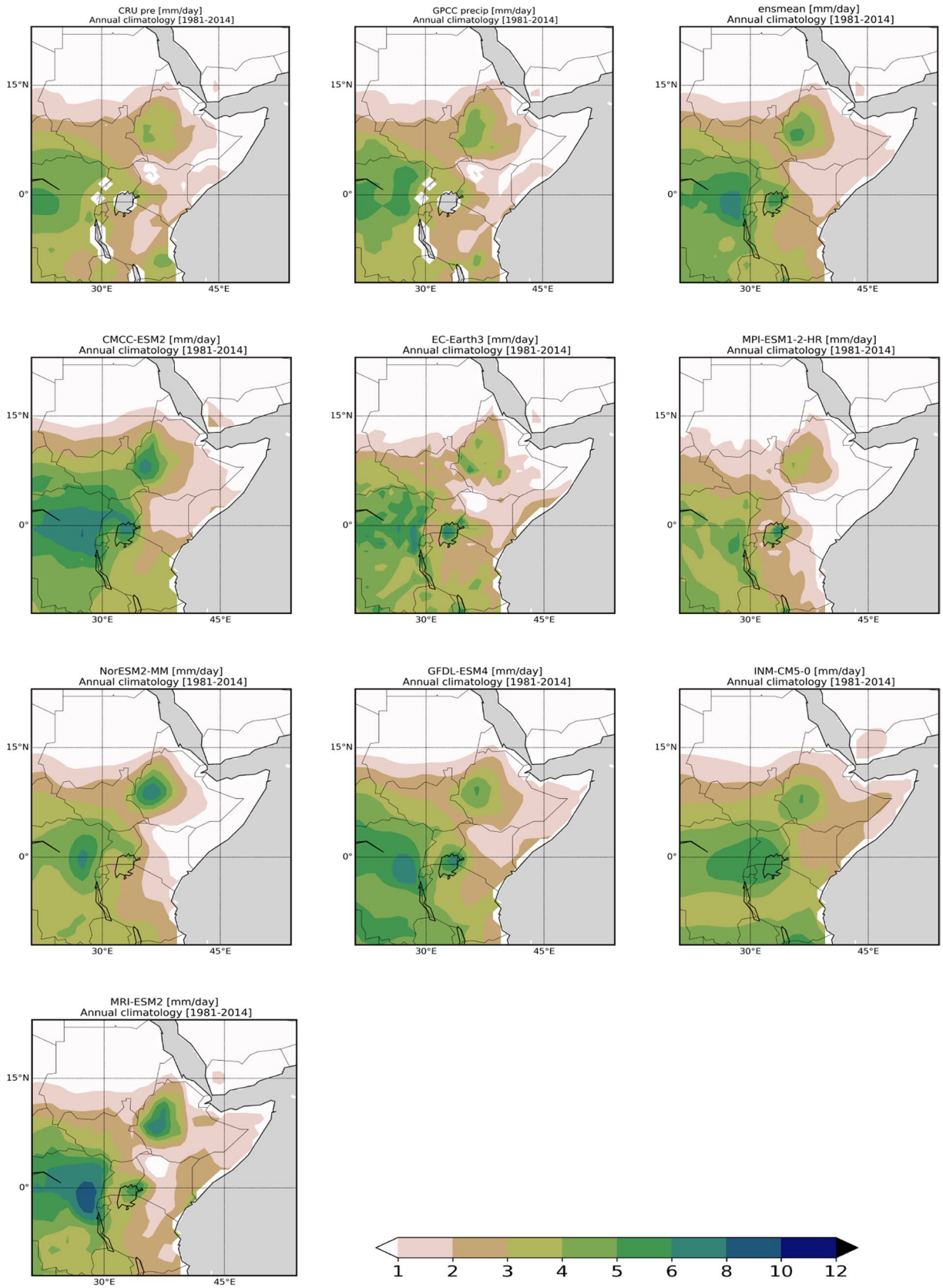

Fig. 1 Spatial pattern of mean annual precipitation (mm/day) from observations, ensemble mean, and individual GCMs for the 1981–2014 period

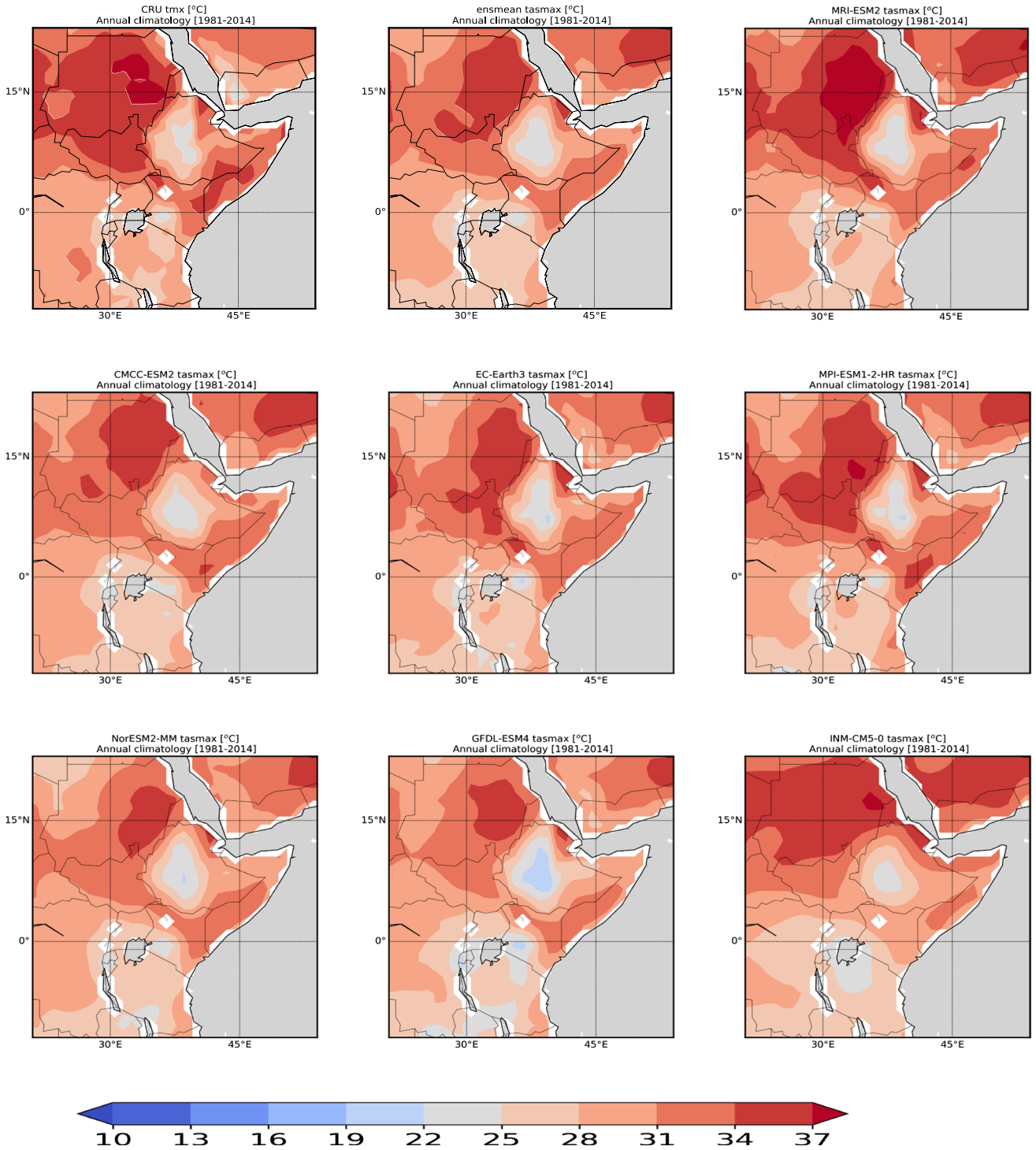

Fig. 2 Spatial pattern of daily maximum temperature (°C) climatology from observations, ensemble model mean, and individual GCMs for the 1981–2014 period

climates over northeastern Sudan and eastern coastal regions and a wetter and cooler climate over Ethiopian highlands and Congo. Most models and the ensemble mean reproduced these characteristics of observed spatial variations well. Few models, however, show biases. For instance, MPI-ESM underestimates the precipitation amount over the Ethiopian highland. CMCC and MRI models, on the other hand, show excessive positive bias over the regions. NorESM and GFDL models show the largest negative bias in representing the intensity of maximum temperature over Sudan.

Figure 3 shows the climatological annual cycles of precipitation and temperature from observation and climate model simulations for two sub-regions that are representative of two different climate regimes-namely northeast and equatorial regimes. The region located in equatorial Africa, shows a bi-modal rainfall pattern corresponding to the northward and southward migration of the Inter-tropical Convergence Zone (ITCZ). These two rainy seasons are spring, the long rainy season, and autumn, the short rainy season. Conversely, the northeast region, comprising Ethiopia, Eritrea, and central Sudan, exhibits a monomodal pattern with the rainy season concentrated during summer. The majority of the models and the ensemble mean capture the annual cycle of precipitation; however, they overestimate precipitation during the short rainy season. The MPI-ESM model underestimates the summer rains over northeast Africa. The annual cycle of daily maximum temperature reveals that the warmest time of the year is in February for the equatorial region and April for the northern regions reaching close to 31 °C and 36 °C, respectively. On the other hand, the coldest time of the year is around December/January for the northern region and around July for the equatorial region, reaching as low as 15 °C at night time. Most of the climate models simulate these observed patterns of the annual cycle, though they systematically underestimate daytime maximum temperature. In particular, the GFDL model shows the highest and consistent cold bias throughout the year.

3.1.2 Extreme climate stressors relevant to livestock

In this section, a description of climatological characteristics of extreme indices as simulated by ensemble means of the CMIP6 models, will be provided. These extreme indices are derived from daily precipitation and daily maximum and minimum temperatures.

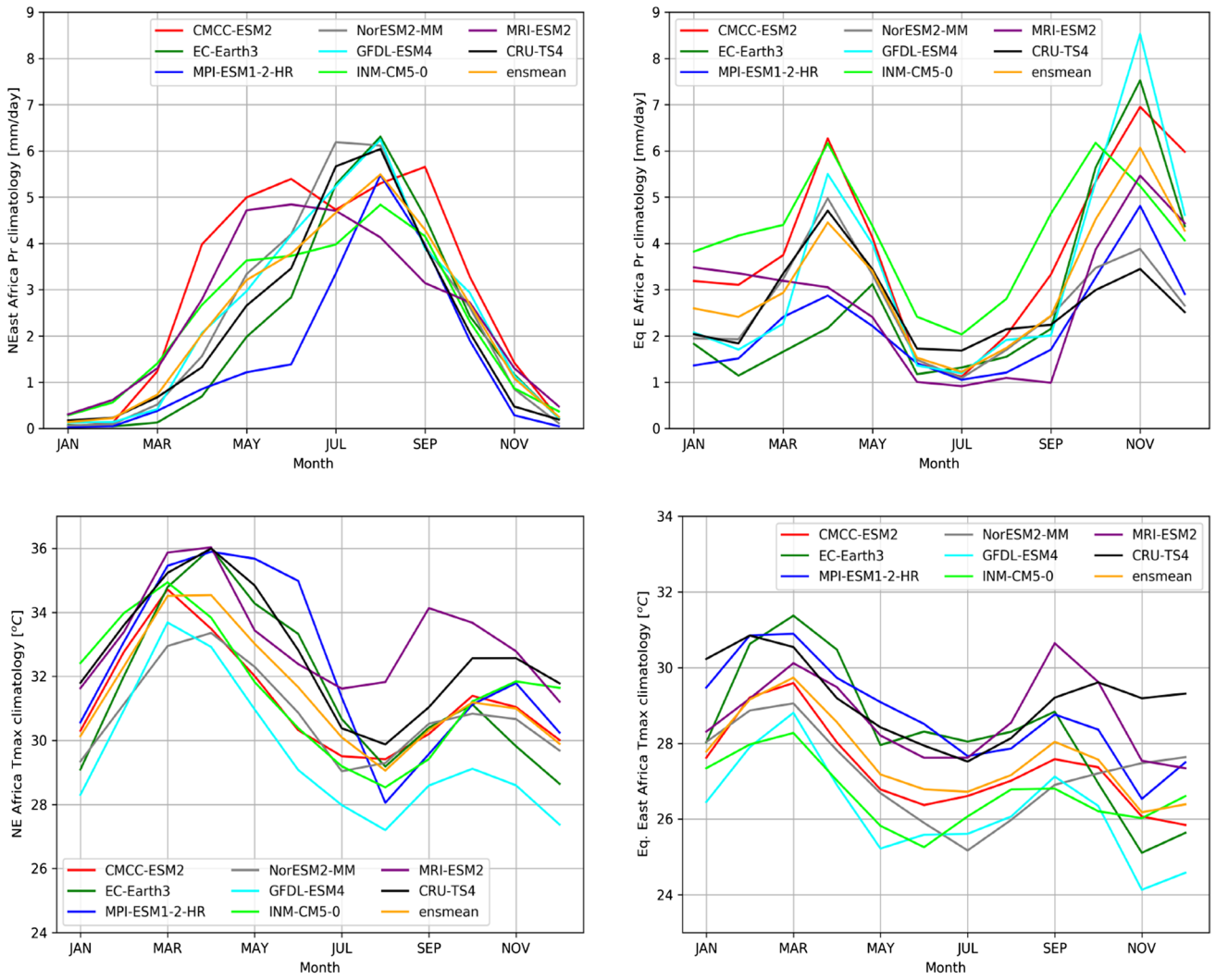

Fig. 3 Observed and simulated annual cycle of precipitation (top row), and daily maximum temperature (bottom row) for monomodal (left) and bimodal (right) regimes

Heavy precipitation related stressors The spatial pattern of high intensity precipitation events from ensemble-mean simulations is shown in Fig. 4. The wet day total precipitation (prcptot) amount greater than 2000 mm is prevalent over Congo and regions near Lake Victoria. On the other hand, the Northern Sudan and coastal areas of Eritrea and Djibouti receive less than 100 mm. The models simulate extreme annual 1-day and 5-day cumulative precipitation events over Lake Victoria, eastern Congo, and Ethiopian highlands. Such extreme precipitation substantially affects livestock via flooding and through increasing the risk of diseases. For instance,

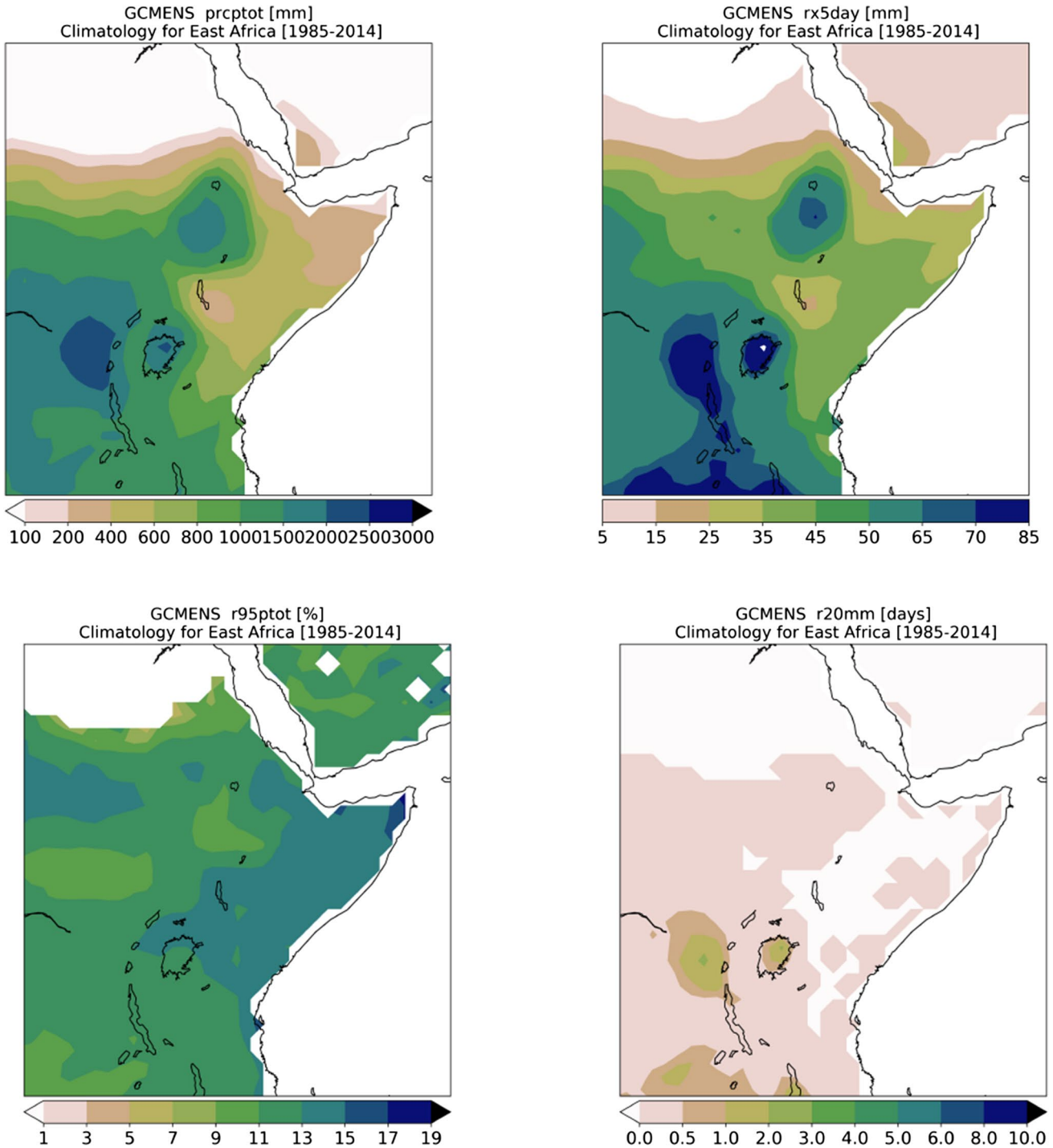

Fig. 4 Spatial distribution of climatological values of extreme precipitation indicators (prcptot, rx5day, r95ptot, and r20mm) from ensemble average of historical simulations

(Little et al. 2001) demonstrated that flood episodes have affected livestock over the Horn of Africa. It should be noted that these extreme precipitation events are often associated with deep convective precipitation that is difficult to be resolved by the models at the 100 km resolution, therefore they are expected to be underestimated in intensity. Similarly, the frequency of very heavy precipitation (RR > 20 mm/day) events is very small. Nevertheless, the model delineates regions affected by the occurrence of such high precipitation events. It is interesting to note that the fraction of 95th and 99th percentile of precipitation to the prcptot (i.e., R95ptot and R99ptot) are higher not only over wet regions but also over the coastal and northeastern regions.

Drought stress indicators While droughts lack a universal definition, its main reflection is a deficit of soil moisture caused mainly by insufficient precipitation. The impact of drought on livestock over East Africa is devastating. According to (Easterling et al. 2007), the 1998/1999 droughts in Ethiopia are reported to have killed up to 62% of the cattle in some areas. In this study, we employ the maximum duration of consecutive dry days (CDD), Standardized Precipitation Index (McKee et al. 1993), and Standardized Precipitation Evapotranspiration Index (Vicente-Serrano et al. 2010) to quantify drought. CDD is the maximum number of consecutive dry days. A dry day is defined as a day when the cumulative daily precipitation value is less than 1 mm. As expected, simulations show fewer numbers of CDD over climatologically wet regions and high numbers of CDD over semi-arid and arid regions. Consequently, the climatological maximum consecutive dry-day (CDD) exhibits high values greater than 300 CDD over the northern part of Sudan and lower values over Congo regions (Fig. 5, left).

SPI has been recommended by the World Meteorological Organization (WMO) to characterize meteorological droughts worldwide (Hayes et al. 2011). It is a relatively simple index, and it is based only on precipitation data to measure the precipitation deficit (drought) or excess rainfall (flood)(Seiler et al. 2002). The SPI measures drought by comparing standardized accumulations of precipitation each month and for a user-specified number of preceding months within a base period. Despite the SPI relying solely on monthly precipitation values, it has been demonstrated to perform well over the East African region by (Ntale and Gan 2003). Another advantage of SPI is that it can be calculated over different time scales to allow the interpretation of drought from monthly to multiyear scale. However, SPI does not consider the effect of evapotranspiration. To address this, SPEI is constructed by employing both precipitation accumulation and potential evapotranspiration, and SPEI has been demonstrated to capture better the characteristics of drought intensity under global warming (Vicente-Serrano et al. 2010). For both SPI and SPEI, we use the 6-month time scale to represent drought. Since SPI and SPEI are standardized values in the historical period, they are by definition close to zero; thus, climatological values of SPI and SPEI do not provide meaningful information. However, the spatial pattern of the frequency of occurrence of drought with threshold less than −1 is shown in Fig. 5. The result indicates that SPEI shows a higher number of droughts over horn and eastern Africa compared to SPI and CDD. These regions of higher occurrence of droughts co-located with higher concentrations of pastoral communities where livestock holds significant cultural value. Higher drought occurrences imply severe water and forage shortages,

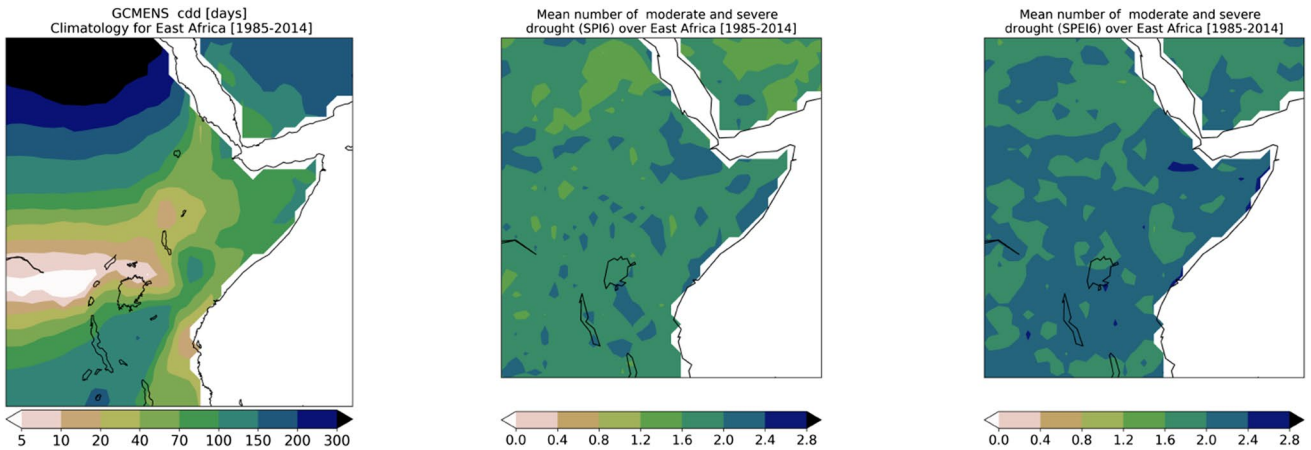

Fig. 5 Spatial distribution of climatological number of dry days (left), number of moderate to severe drought events from SPI6 (middle) and SPEI6 (right) for the present-day climatological period from ensemble average model simulation

which directly affect livestock health, productivity and mortality due to starvation and malnutrition (Leweri et al. 2021).

Heat stress related indicators In general, the ensemble mean simulation indicates a strong spatial gradient of heat stress, displaying an intense warm spell, amplitude, and heat wave frequency in the northern part of the domain, including Sudan and Saudi Arabia, and lower values over East African highlands (Fig. 6). The above regions exhibiting higher heat stress indicators are not conducive for livestock production as heat stress is adversary affecting animal reproduction or fertility, milk production, health, fitness and longevity, and the level of water consumption

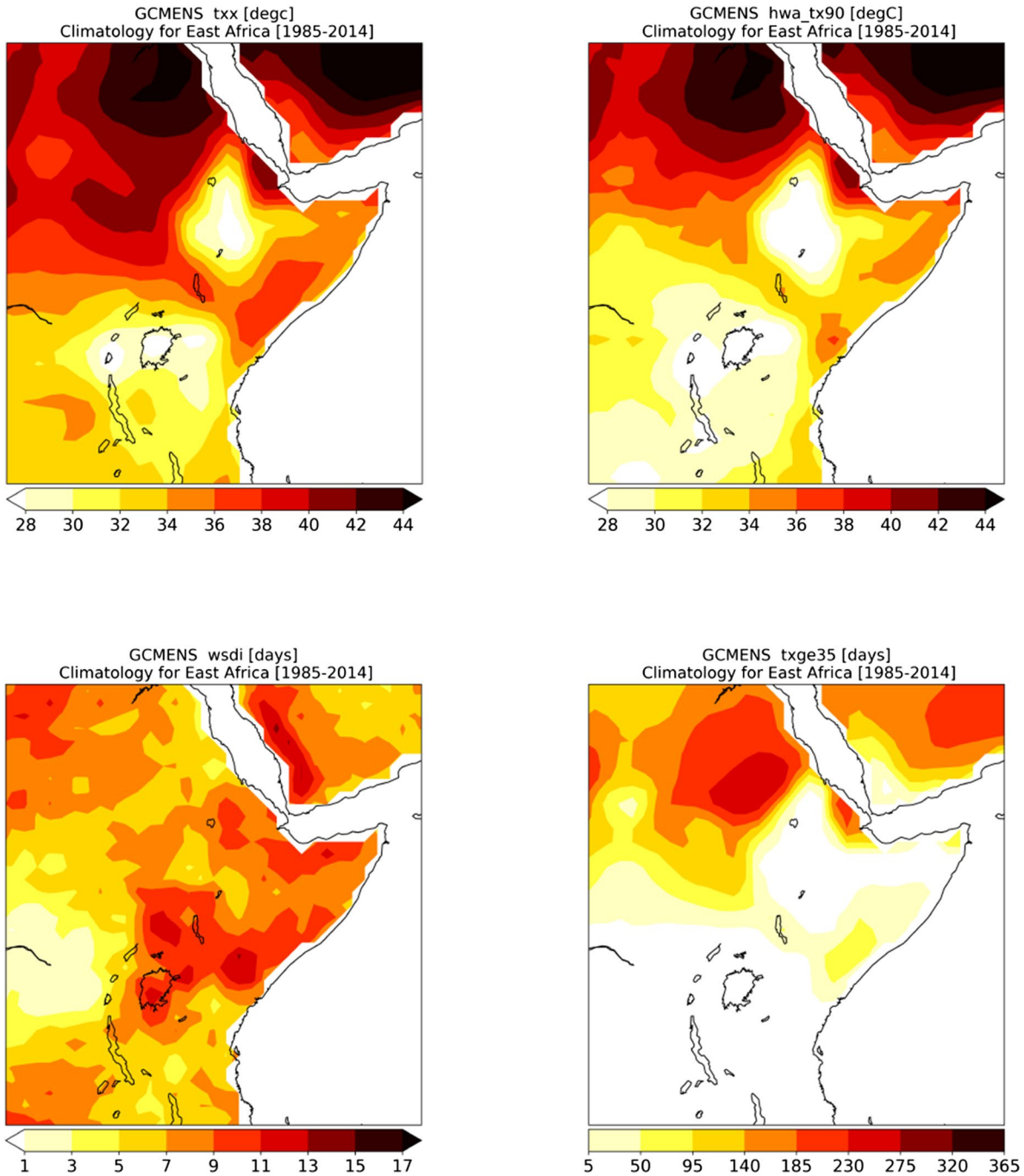

Fig. 6 Spatial distribution of present-day climatological values of heat stress indicators (Txx, HWA, WSDI, and Txge35) from ensemble average model simulation

(Rojas-Downing et al. 2017; Easterling et al. 2007). The spatial pattern of warm spell duration does not follow the pattern of heat wave amplitude and intensity: the values of the warm spell duration are higher instead over Lake Victoria and central Kenya.

3.1.3 Present-day agro-climatological classification

Figure 7 shows present-day agro-climatic regions based on ensemble mean CMIP6 climate model output. It can be seen that the region has been divided into the following agro-climatic regions. Semi-Arid: semi-arid regions are found in eastern and northern parts of Ethiopia, central and eastern Kenya, southern Sudan, and most of Somalia. Arid: Most of the Arid regions are in Sudan, middle-east and Somaliland. Other smaller areas include Eritrea, northeastern Ethiopia, and a small region of northern Kenya. Sub-Humid: This zone occupies most of Tanzania, western and southern Kenya, western and central Ethiopia and the whole of South Sudan. Humid: This zone mainly covers Congo, Uganda, western Kenya, and southwestern Ethiopia. The classification of these zones are useful to provide insights for developing targeted interventions that enhance agricultural resilience and sustainability.

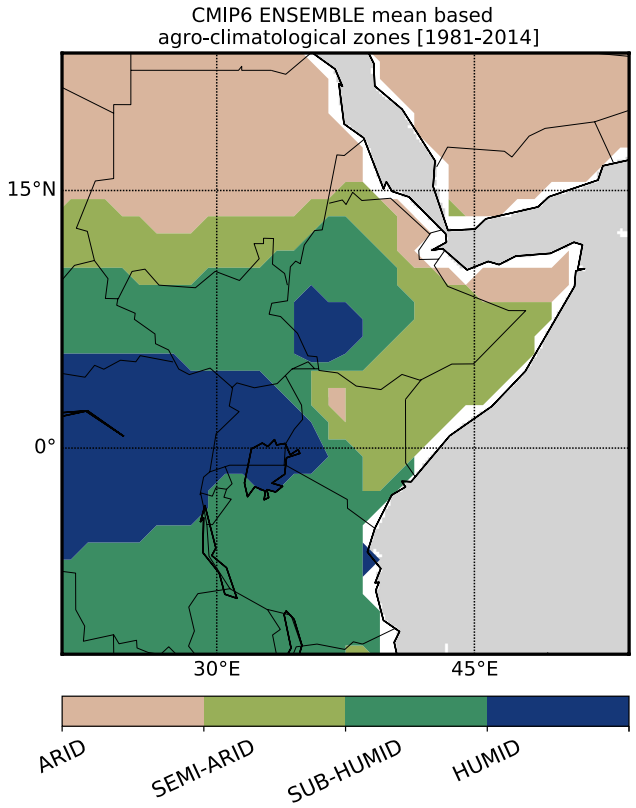

Fig. 7 CMIP6 ensemble mean based agro-climatic zones for present-day climate

3.2 Projected changes in mean and extreme climate, and agro-climatic zones

In this section, we discuss changes in the extreme indices for the future horizons with respect to the historical base period. We present the changes as spatial maps of the ensemble average changes (Figs. 8, 9, 10, 11, 12, and 13).

The projected changes in annual mean precipitation and temperature climatology for the far-future period (2071–2100) compared to present-day is shown in Supplementary materials Figure S1. As expected, climatology of annual mean daily maximum temperature is projected to increase throughout the domain, however the smallest changes are over the equatorial region and the change increases as we go to higher latitude. The largest temperature changes are observed over the northern part of the domain that includes northern Sudan and over the Arabian Peninsula. Annual mean precipitation is also projected to increase over most of the eastern Africa region with the highest increase observed over regions surrounding Lake Victoria, Uganda, and western Ethiopia. The results also confirm that the projection with the SSP585 scenario shows more severe changes (e.g., larger increases in temperature and precipitation) compared to the SSP245 scenario for many regions.

3.2.1 Changes in heavy precipitation indices (flood indicators)

As shown in Figs. 8 and 9, most of the indices related to high precipitation extremes show increases in future climate, because of increases in water vapor brought about by future warming (Collins et al. 2013). For PRCPtot, the projected change shows positive values over most parts of the domain with the exception of the southern and northern part of the domain. Compared with the SSP245 scenario, more pronounced increases in RX5day, R20mm, and R95pTot are projected over most of the domains under the SSP585 scenario. These results imply that East Africa will experience an increase in both the intensity (RX5day, R95pTot, PRCPtot) and frequency (R20mm) of heavy precipitation events due to anthropogenic climate change. This implies more chances of severe and prolonged flooding events. This projected increase in heavy precipitation events over the region is consistent with the result of Tegegne et al. (2021); Ayugi et al. (2021a, b); Ngoma et al. (2022). From the impact side, it is expected that the projected increase in heavy precipitation and subsequent flooding can disrupt traditional grazing patterns for livestock. It can also increase the risk of water-logging, and create conducive conditions to the spread of diseases among livestock which further complicate livestock management (Munsey et al. 2021).

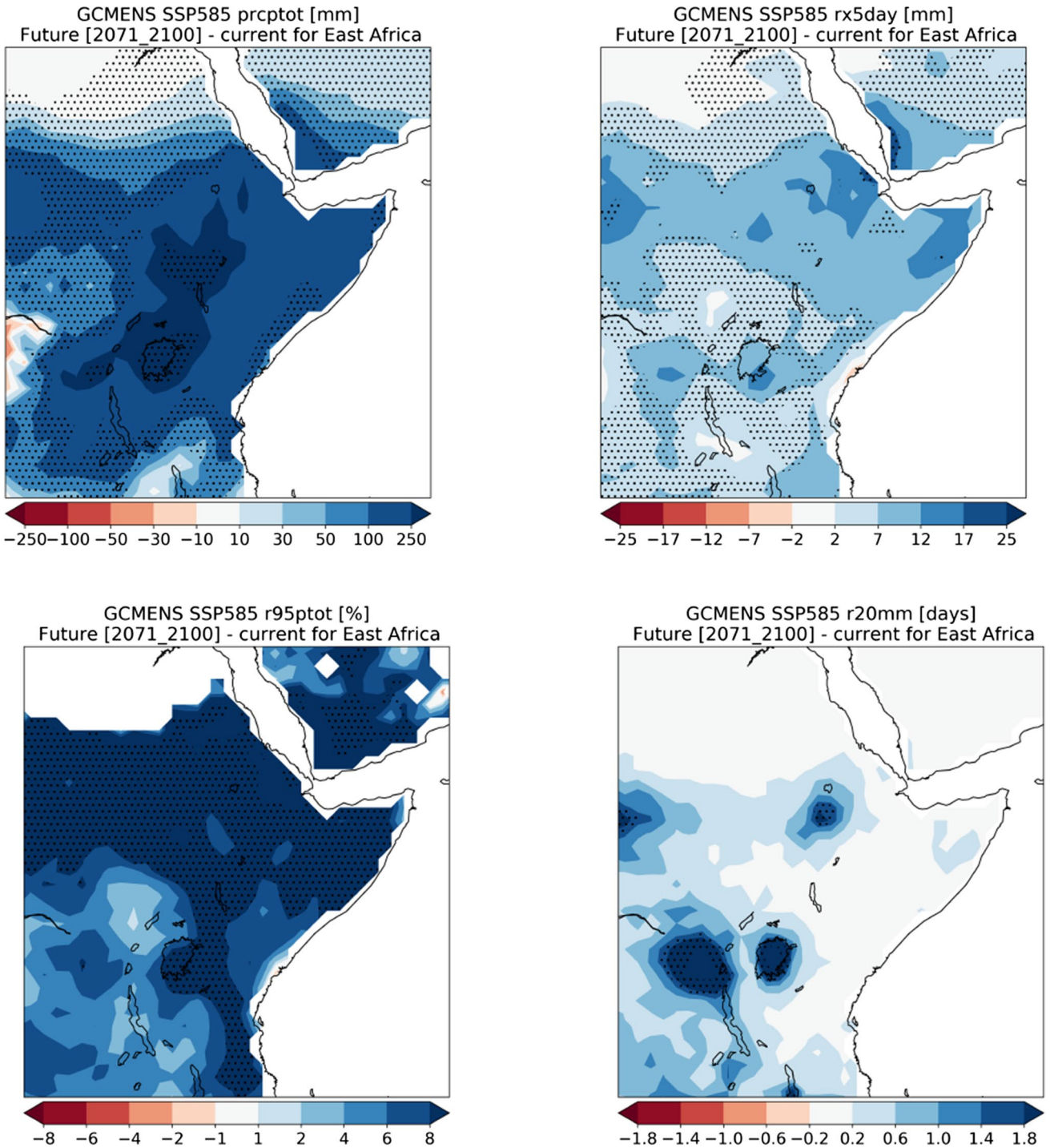

Fig. 8 Spatial distribution of projected changes in extreme high precipitation indicators for far future based on SSP585 scenarios

3.2.2 Changes in drought indicators

Figure 10 presents the projected changes in the frequency of drought occurrence as measured by SPI6, SPEI6, and duration of the longest dry period (CDD) for the two emission scenarios. For SPI and SPEI, drought occurrences are defined when the SPI value is less than −1. The two drought stress indicators (SPEI6 and CDD) are showing significant intensification of droughts for most parts of the region in the future climate, particularly when the SSP585 scenario is chosen. SPI6, on the other hand, follows the pattern of mean precipitation where intensification drought

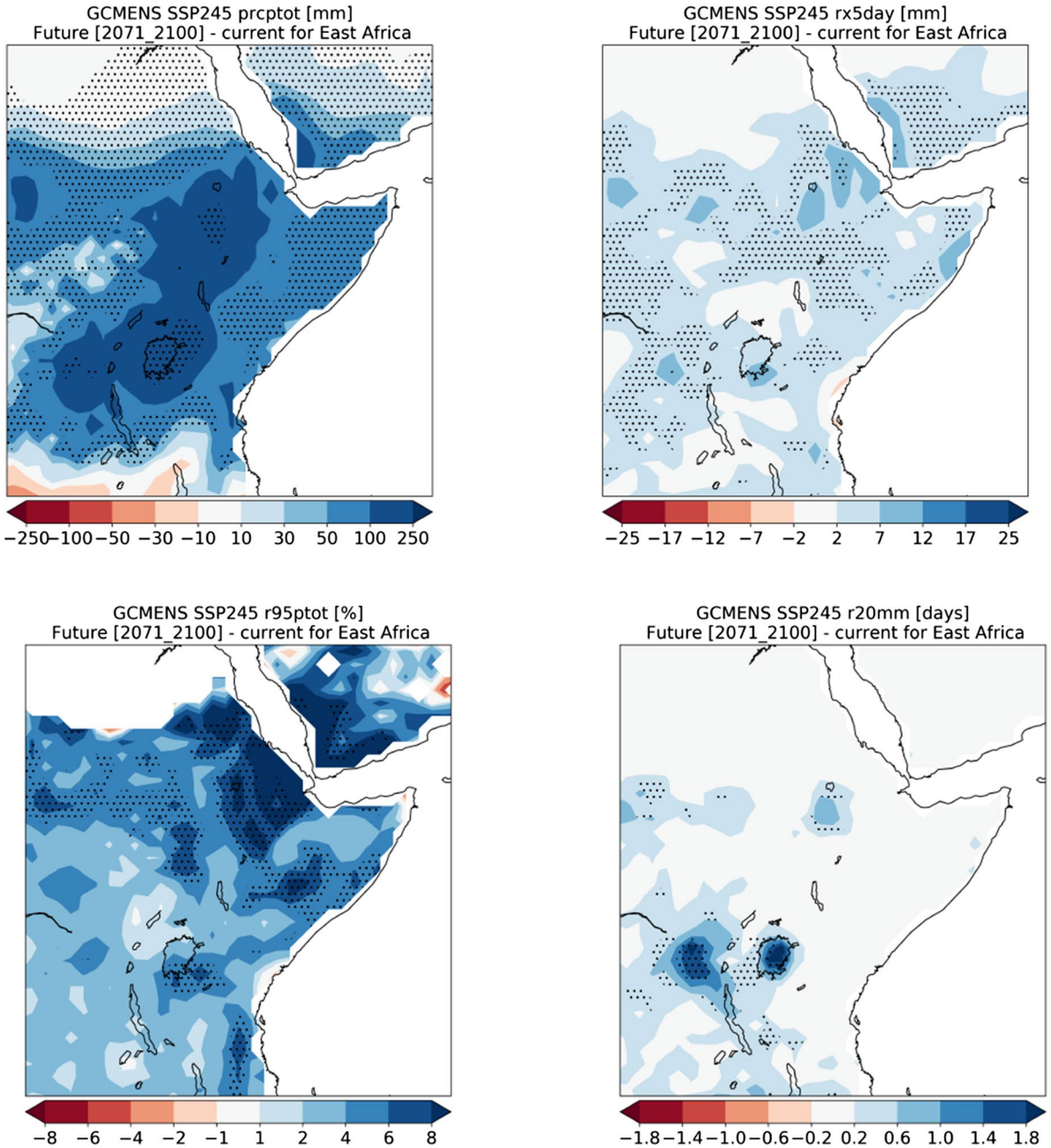

Fig. 9 Spatial distribution of projected changes in extreme high precipitation indicators for the far future based on SSP245 scenarios

does not include the central and northeast region. This is because the SPI6 is derived from precipitation data alone and does not consider the increase in evapotranspiration. Again, the degree of intensification of drought in the future climate is weakened when the SSP245 scenario is considered.

The above results suggest that with increased GHGs, the risk of drought and consecutive dry days for some East African regions such as parts of Somalia, Eastern Ethiopia and northern Kenya is either neutral or slightly declining.. On the other hand, the increase in SPEI and CDD, over the southern domain such as over Tanzania suggests the intensification of drought. The increase in drought over Tanzania is consistent with several previous studies (e.g., Ayugi et al. 2021a, b; Haile et al. 2020; Nyembo et al. 2022). The increased GHG-induced change of a hydrologic cycle regime towards few intense rainfall days (as discussed in Sect. 4.1) but less number of rainy days (increased number of dry days as shown in Fig. 11) is consistent with the result of previous studies (e.g., Giorgi

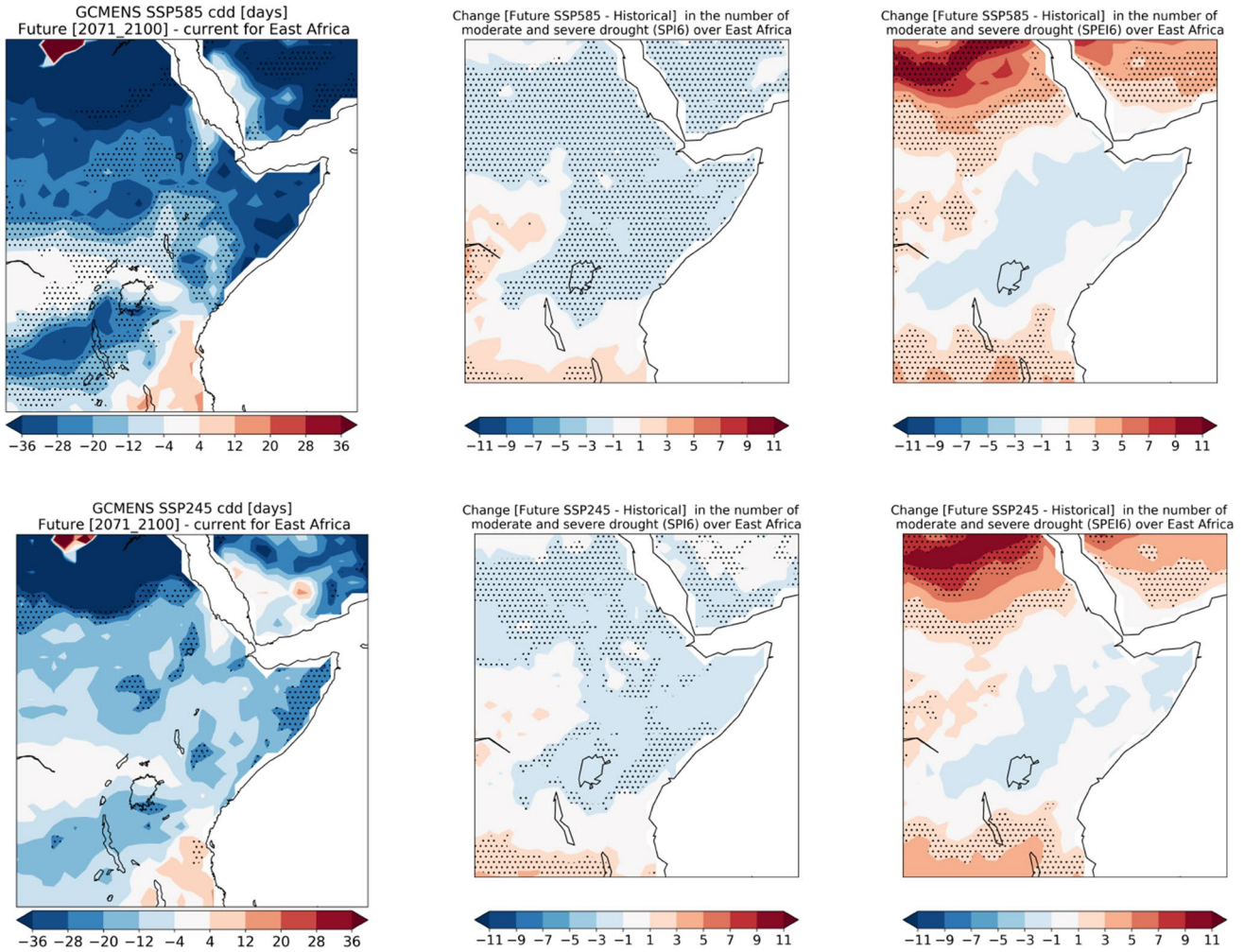

Fig. 10 Spatial pattern of projected changes in CDD (in days, left), in number of moderate and severe droughts as measured by SPI6 (in months, middle) and SPEI6 (in months, right) for the far future period under SSP585 (top) and SSP245 (bottom) scenarios

et al. 2014; Giorgi et al. 2011), and it will have critical implications for the local water resources management, and agricultural production.

3.2.3 Changes in heat stress indicators

Figures 11 and 12 show the ensemble average changes (future minus historical) for the heat stress indicator indices. It is evident that most areas exhibit positive values for all heat stress indices. As expected, the frequency, duration, and intensity of warm spells and heat waves increase when the SSP585 scenario is considered. While all heat stress indicators are projected to increase in future climates, the highest and most significant increase is noted for the warm spell duration index (WSDI). The warm spell duration is projected to increase by greater than 300 days under the SSP585 emission scenario. This amplification of all heat stress indicators over the region in future climate is inline with the conclusion of Asefi-Najafabady et al. (2018); Das et al. (2023); Fotso-Nguemo et al. (2023) and Thornton et al. (2021).

3.2.4 Future agro-climatological zones

Spatial distribution of future agro-climatic zones, presented in Fig. 13, indicates that semi-arid regions in Somalia are projected to expand to the Somali land, and regions of humid areas in Uganda and Congo are projected to expand into the southern part of South Sudan to connect to the humid area in the southwest Ethiopia.

Figure 13 (bottom panel) also shows that the sub-humid regions in southern Tanzania are retreating northward, leaving the region to a semi-arid zone. These results indicate that climate change will shift the sub-humid regions to semi-arid over the southern part of the domain, whereas the arid

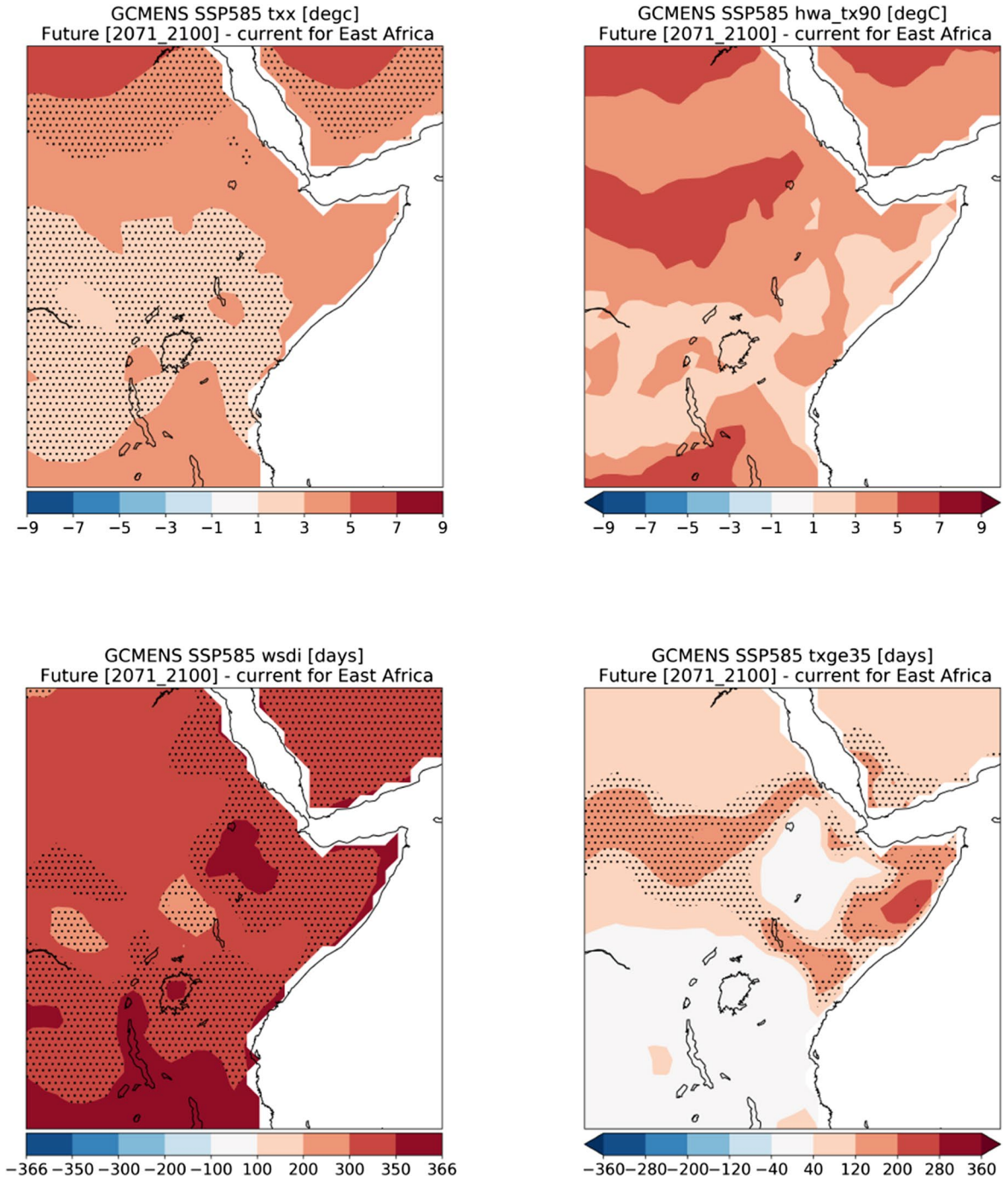

Fig. 11 Spatial pattern of projected changes to heat stress intensity (top row) and frequency (bottom row) indicators for far future period under SSP585 emission scenario

regions in the horn are projected to shrink. The climatic shift from arid to semi-arid and from sub-humid to humid is consistent with the projected increase in precipitation in the CMIP6 dataset over East Africa. These results imply that future adaptation strategies should consider changes in agro-ecological conditions, since effective adaptation strategies should be tailored to specific agro-ecological zones.

4 Conclusion and recommendations

A detailed regional analysis of climate change's impact on the frequency and intensity of extreme climate events and the changes in the major agro-climatic zones is of paramount importance to the agricultural sector in general and to livestock production in particular. To this

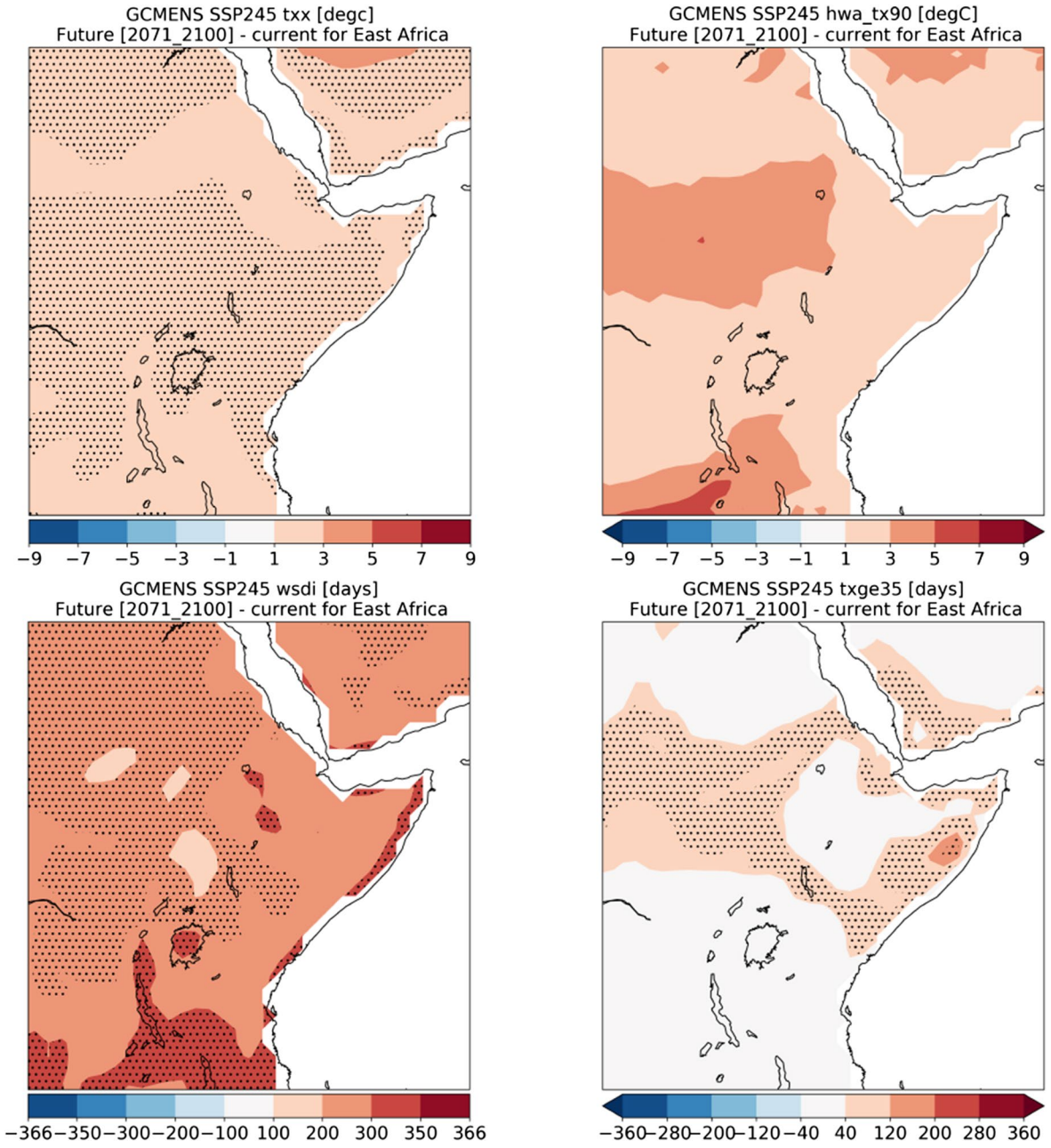

Fig. 12 Spatial pattern of projected changes to heat stress intensity (top row) and frequency (bottom row) indicators for far future under SSP245 scenario

end, analysis of present-day and future projected changes to agro-climatic zones over East Africa and sector-specific extreme climate indices has been carried out using ensembles of selected climate models from CMIP6. For future climate, SSP245 and SSP585 emission scenarios are considered. To assess the role of climate change on extremes, a subset of indices are selected from sector-specific extreme climate indices. These indices are PRCPtot, RX5day, R95Ptot, R20mm, CDD, SPI, SPEI, WSDI, TXx, TXge35 and HWA.

A comparison of the present-day model simulations with observational datasets reveals that the ensemble mean is able to simulate the basic characteristics of mean climate variables. In particular, the ensemble model averaged reasonably simulates both the spatial distribution and annual cycle of precipitation and temperature, even if the model showed some biases in simulating short rain season (OND) precipitation over East Africa equatorial regions.

Projected changes related to extremes reveal that the frequency and intensity of heavy extreme precipitation events

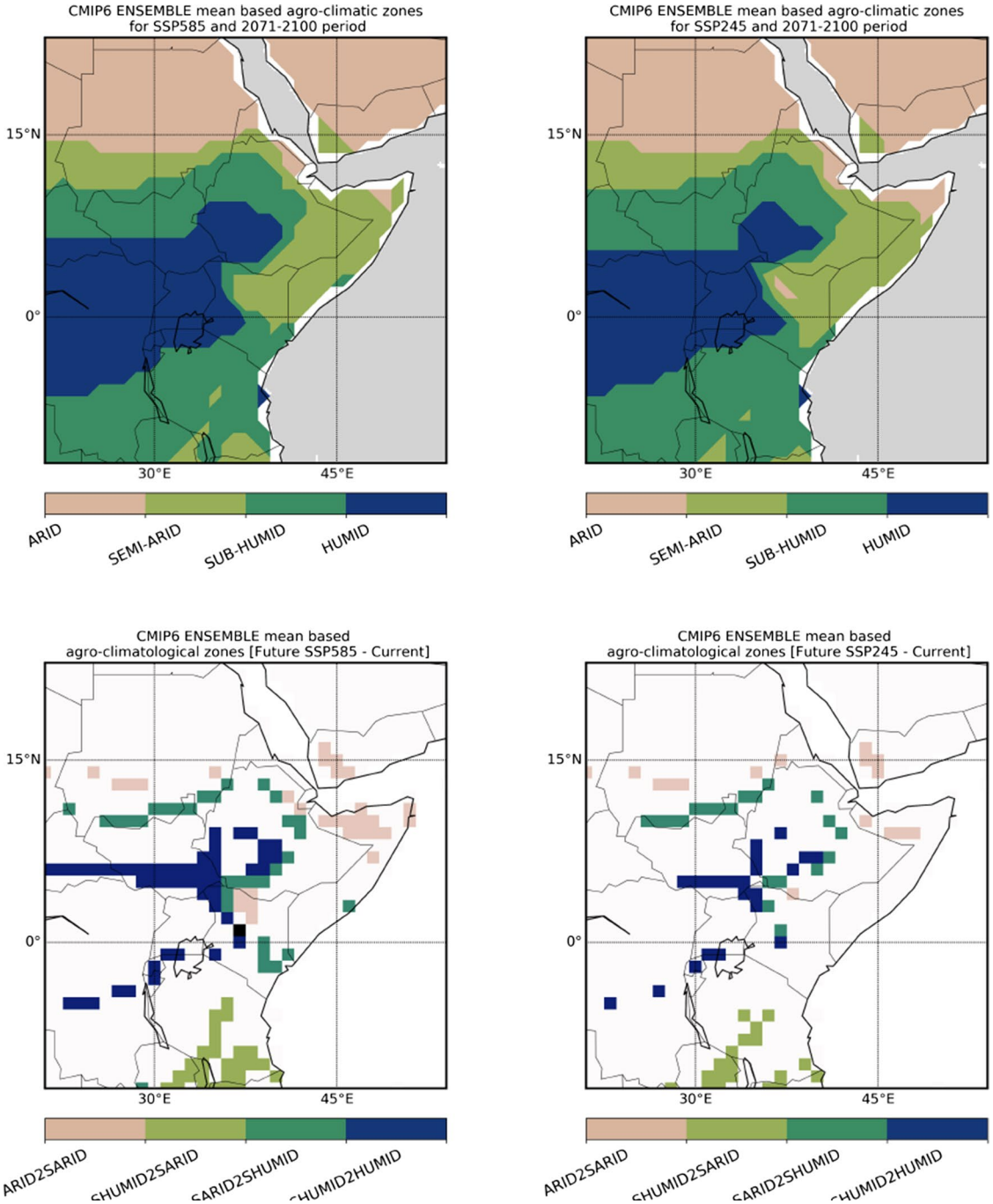

Fig. 13 Future agro-climatic zones for the far future (2071–2100) period based on SSP585 (left) and SSP245 (right) emission scenario. The bottom panel shows the changes/shifts in the agro-climatic zone corresponding to SSP585 (bottom left) and SSP245 (bottom right)

(RX5day, R20mm, R95Ptot, etc.) are expected to increase over most of the Horn of Africa. The increase in intense precipitation could lead to a rise in flood hazards in areas where intense rain typically triggers inundations. As a result, crop and livestock production will likely be at high risk in the region. On the other hand, drought indicators suggest that the frequency of extreme dry events associated with drought will likely decrease over most parts of East Africa except over some regions such as over Tanzania.

Projections show that all heat stress indicators will be amplified in warmer future climate. In particular, a significant increase is projected for the warm spell duration index (WSDI) among the heat stress indicators. The warm spell duration is projected to increase by about 245 days over

Ethiopian highlands by the end of the century (2071–2100) under the SSP585 emission scenario. As this amplification of heat stress is leading to a decrease in livestock production (Rahimi et al. 2021), adaptation that focuses towards heat-tolerance breeding will be paramount to the livestock sector.

As different agro-climate types are associated with a certain agricultural production system (Fischer et al. 2021), the redistribution of climate types suggests concomitant changes in the agricultural production system. Our analysis indicates that the percentage of arid regions is projected to decline in Somalia in future warmer climates. The results also highlight that the area covered by humid agro-climatic types is projected to increase and cover most of the southern part of South Sudan in future periods. The sub-humid agro-climate types in historical periods over southern Tanzania are noted to be replaced by semi-arid agro-climate in future climates. Our analysis indicated that the extent of change in the agro-climate zone is sensitive to the emission scenario followed and is stronger under SSP585. This implies that stakeholders and practitioners should ensure that future adaptive measures consider the shift in agroecological zones.

While this study makes use of ensembles of CMIP6 GCMs which have relatively higher resolutions i.e., ~ $1° \times 1°$ degree, it is still coarser for extracting and using local and regional information. Therefore, future studies with downscaled and high resolution climate projection would be helpful for local and sub-regional decision making processes.

Supplementary information The online version contains supplementary material available at https://doi.org/10.1007/s00704-025-05405-2.

Acknowledgements We would like to thank the modeling groups listed in Table 1 which are available at https://esgf-node.llnl.gov/projects/cmip6/. This research paper was made possible through generous support from multiple projects. We gratefully acknowledge the financial support from the European Union Department for International Partnerships (INTPA) that funded the LEG4DEV DESIRA project (https://leg4dev.org/); the Australian Centre for International Agricultural Research (ACIAR) and the Accelerating Impacts of CGIAR Climate Research for Africa (AICCRA). AICCRA aims to deliver a climate-smart African future driven by science and innovation in agriculture and is supported by a grant from the International Development Association (IDA) of the World Bank. Explore our work at https://aiccra.cgiar.org/. GTD is currently affiliated with Environment and Climate Change Canada.

Author contributions Conceptualized, T.D.D., G.T.D., and T.B.J; methodology, T.D.D. and G.T.D.; formal analysis, G.T.D.; writing—original draft, T.D.D., G.T.D.; writing—review and editing, T.D.D., G.T.D., C.D., T.B.J., and D.S.; supervision, G.T.D., T.D.D., C.D., T.B.J., and D.S.; All authors have read and agreed to the published version of the manuscript.

Funding T.D.D. acknowledges funding support from the European Union Department for International Partnerships (INTPA) that funded the LEG4DEV DESIRA project (https://leg4dev.org/; Grant Number: FOOD/2020/418–90). This research was also funded by the Australian Centre for International Agricultural Research (ACIAR) and the International Development Association (IDA) of the World Bank to the Accelerating Impact of CGIAR Climate Research for Africa (AICCRA) project.

Data availability No datasets were generated or analysed during the current study.

Code availability Not applicable.

Declarations

Ethics approval Not applicable.

Consent to participate Not applicable.

Consent for publication Not applicable.

Competing interests The authors declare no competing interests.

References

Akinsanola AA, Ongoma V, Kooperman GJ (2021) Evaluation of CMIP6 models in simulating the statistics of extreme precipitation over Eastern Africa. Atmos Res 254(June):105509. https://doi.org/10.1016/j.atmosres.2021.105509

Alexander L and Herold N (2016) ClimPACT2: indices and software

Anyah RO, Semazzi FHM (2004) Simulation of the sensitivity of lake Victoria Basin climate to lake surface temperatures. Theoret Appl Climatol 79:55–69

Asefi-Najafabady S, Vandecar KL, Seimon A, Lawrence P, Lawrence D (2018) Climate change, population, and poverty: vulnerability and exposure to heat stress in countries bordering the great lakes of Africa. Clim Change 148:561–573

Ayugi B, Dike V, Ngoma H, Babaousmail H, Mumo R, Ongoma V (2021a) Future changes in precipitation extremes over East Africa based on CMIP6 models. Water 13(17):2358

Ayugi B, Ngoma H, Babaousmail H, Karim R, Iyakaremye V, Lim KTC, Sian K, Ongoma V (2021b) Evaluation and projection of mean surface temperature using CMIP6 models over East Africa. J Afr Earth Sc 181(September):104226. https://doi.org/10.1016/j.jafrearsci.2021.104226

Bahaga TK, Mengistu Tsidu G, Kucharski F, Diro GT (2015) Potential predictability of the sea-surface temperature forced equatorial East African short rains interannual variability in the 20th century. Q J R Meteorol Soc 141(686):16–26. https://doi.org/10.1002/qj.2338

Beguería S, Vicente-Serrano SM, Angulo-Martínez M (2010) A multiscalar global drought dataset: the SPEIbase: a new gridded product for the analysis of drought variability and impacts. Bull Am Meteor Soc 91(10):1351–1354

Cherchi A, Fogli PG, Lovato T, Peano D, Iovino D, Gualdi S, Masina S, Scoccimarro E, Materia S, Bellucci A, Navarra A (2019) Global mean climate and main patterns of variability in the CMCC-CM2 coupled model. J Adv Model Earth Syst 11(1):185–209

Collins M, Knutti R, Arblaster J, Dufresne J-L, Fichefet T, Friedlingstein P, Gao X, Gutowski WJ, Johns T, Krinner G, Shongwe M, Tebaldi C, Weaver AJ, & Wehner M (2013) Chapter 12 - long-term climate change: projections, commitments and irreversibility. In IPCC (ed) Climate change 2013: the physical science basis. IPCC Working Group I Contribution to AR5, Cambridge University Press

Das P, Zhang Z, Ghosh S, Jianzhong Lu, Ayugi B, Ojara MA, Guo X (2023) Historical and projected changes in extreme high temperature events over East Africa and associated with meteorological conditions using CMIP6 models. Glob Planet Chang 222:104068

Diro GT, Grimes DIF, Black E (2011a) Teleconnections between Ethiopian summer rainfall and sea surface temperature: part iobservation and modelling. Clim Dyn 37(1):103119. https://doi.org/10.1007/s00382-010-0837-8

Diro GT, Grimes DIF, and Black E (2011) Large scale features affecting Ethiopian rainfall. Afr Climate Climate Chang: Phys Soc Polit Perspect 13–50

Dosio A, Jury MW, Almazroui M, Ashfaq M, Diallo I, Engelbrecht FA, Klutse NAB et al (2021) Projected future daily characteristics of African precipitation based on global (CMIP5, CMIP6) and regional (CORDEX, CORDEX-CORE) climate models. Clim Dyn 57(11):3135–3158

Easterling WE, Aggarwal PK, Batima P, Brander KM, Lin Erda S, Howden M, Kirilenko A et al (2007) Food, fibre and forest products. Clim Change 2007:273–313

Fischer G, Nachtergaele O, Velthuizen F, Chiozza VTH, Franceschini F, Henry G, Muchoney M, Tramberend DS (2021) Global agro-ecological zones v4 – model documentation. Food Agric Org

Fotso-Nguemo, Thierry C, Weber T, Diedhiou A, Chouto S, Vondou DA, Rechid D and Jacob D (2023) Projected impact of increased global warming on heat stress and exposed population over Africa. Earth's Future 11(1): e2022EF003268

Funk C, Peterson P, Landsfeld M, Pedreros D, Verdin J, Shukla S, Husak G et al (2015) The climate hazards infrared precipitation with stations - a new environmental record for monitoring extremes. Sci Data. https://doi.org/10.1038/sdata.2015.66

Giorgi F, Im E-S, Erika Coppola NS, Diffenbaugh XJG, Mariotti L, Shi Y (2011) Higher hydroclimatic intensity with global warming. J Clim 24(20):5309–5324

Giorgi F, Coppola E, Raffaele F, Diro GT, Fuentes-Franco R, Giuliani G, Mamgain A, Llopart MP, Mariotti L, Torma C (2014) Changes in extremes and hydroclimatic regimes in the CREMA ensemble projections. Clim Change 125:39–51

Gleixner S, Keenlyside N, Viste E, Korecha D (2017) The El Niño effect on Ethiopian summer rainfall. Clim Dyn 49(5):1865–1883. https://doi.org/10.1007/s00382-016-3421-z

Gutjahr O, Putrasahan D, Lohmann K, Jungclaus J, von Storch J-S, Brüggemann N, Haak H, & Stössel A (2018) Max planck institute earth system model (MPI-ESM1.2) for the high-resolution model intercomparison project (HighResMIP). Geosci Model Dev. https://doi.org/10.5194/GMD-12-3241-2019

Haile, Gebremedhin G, Qiuhong T, Seyed-Mohammad H-M, Liu X, Gebremicael TG, Guoyong L, Asfaw K, Xu X, and Yun X (2020) Projected impacts of climate change on drought patterns over east Africa. Earth's Future 8(7): e2020EF001502

Hargreaves GH, Samani ZA (1985) Reference crop evapotranspiration from temperature. Appl Eng Agric 1(2):96–99

Harris I, Osborn TJ, Jones P, and Lister D (2020) Version 4 of the CRU TS monthly high-resolution gridded multivariate climate dataset. Sci Data 7(1). https://doi.org/10.1038/s41597-020-0453-3

Hayes M, Svoboda M, Wall N, Widhalm M (2011) The lincoln declaration on drought indices: universal meteorological drought index recommended. Bull Am Meteor Soc 92(4):485–488

Held IM, Guo H, Adcroft A, Dunne JP, Horowitz LW, Krasting J, Shevliakova E, Winton M, Zhao M, Bushuk M, Wittenberg AT, Wyman B, Xiang B, Zhang R, Anderson W, Balaji V, Donner L, Dunne K, Durachta J,… Zadeh N (2019) Structure and performance of GFDL's CM4.0 climate model. J Adv Model Earth Syst 11(11):3691–3727

Hersbach H, Bill B, Berrisford P, Horányi A, Sabater JM, Julien N, Raluca R et al (2019) Global reanalysis: goodbye ERA-interim, hello ERA5. ECMWF Newslett

Fairman Jr, Jonathan G, Udaysankar SN, Sundar AC, and Thomas M (2011) Land use change impacts on regional climate over Kilimanjaro. J Geophy Res: Atmos 116(D3)

Kolstad, Wilhelm E, Macleod D, and Demissie TD (2021) Drivers of subseasonal forecast errors of the East African short rains. Geophys Res Lett 48(14):e2021GL093292

Kruska RL, Reid RS, Thornton PK, Henninger N, Kristjanson PM (2003) Mapping livestock-oriented agricultural production systems for the developing world. Agric Syst 77(1):39–63

Leweri CM, Msuha MJ, Treydte AC (2021) Rainfall variability and socio-economic constraints on livestock production in the Ngorongoro Conservation Area, Tanzania. SN Appl Sci 3:1–10

Li L, Li W, Ballard T, Sun Ge, Jeuland M (2016) CMIP5 CMIP5 model simulations of Ethiopian Kiremt-Season precipitation: current climate and future changes. Clim Dyn 46(9):2883–2895. https://doi.org/10.1007/s00382-015-2737-4

Little PD, Mahmoud H, Layne D, Coppock (2001) When deserts flood: risk management and climatic processes among East African pastoralists. Climate Res 19(2):149–159

Massonnet F, Ménégoz M, Acosta M, Yepes-Arbós X (2020) Replicability of the EC-earth3 earth system model under a change in computing environment. Geosci Model Dev 13:1165–1178

McKee TB (1995) Drought monitoring with multiple time scales. Proceedings of 9th conference on applied climatology, Boston. https://ci.nii.ac.jp/naid/10028178079/

McKee, Thomas B, Doesken NJ, Kleist J et al (1993) The relationship of drought frequency and duration to time scales. In Proceedings of the 8th Conference on Applied Climatology, Vol. 17. California, pp 179–83. 22

Munsey A, Mwiine FN, Ochwo S, Velazquez-Salinas L, Ahmed Z, Maree F, Rodriguez LL, Rieder E, Perez A, Dellicour S, VanderWaal K (2021) Phylogeographic analysis of foot-and-mouth disease virus serotype O dispersal and associated drivers in East Africa. Mol Ecol 30(15):3815–3825

Ngoma H, Ayugi B, Onyutha C, Babaousmail H, Lim KTC, Sian K, Iyakaremye V, Mumo R, Ongoma V (2022) Projected changes in rainfall over Uganda based on CMIP6 models. Theoret Appl Climatol 149(3):1117–1134

Ntale HK, Gan TY (2003) Drought indices and their application to East Africa. Int J Climatol: A J Royal Meteorol Soc 23(11):1335–1357

Nyembo LO, Mwabumba M, Jahangeer J, Kumar V (2022) Historical and projected spatial and temporal rainfall status of Dar Es Salaam, Tanzania, from 1982 to 2050. Front Environ Sci 10:1025760

O'neill, Brian C, Tebaldi C, Detlef P,Vuuren V, Eyring V, Friedlingstein P, Hurtt G, Knutti R et al (2016) The scenario model intercomparison project (ScenarioMIP) for CMIP6. Geosci Model Dev 9(9):34613482. https://doi.org/10.5194/gmd-9-3461-2016

Ongoma V, Chen H, Gao C (2018) Projected changes in mean rainfall and temperature over East Africa based on CMIP5 models. Int J Climatol 38(3):1375–1392

Otieno VO, Anyah RO (2013) CMIP5 simulated climate conditions of the greater horn of Africa (GHA). Part II: projected climate. Clim Dyn 41:2099–2113

Rahimi J, Mutua JY, Notenbaert AMO, Marshall K, Butterbach-Bahl K (2021) Heat stress will detrimentally impact future livestock production in East Africa. Nature Food 2(2):88–96

Rojas-Downing MM, Pouyan Nejadhashemi A, Harrigan T, Woznicki SA (2017) Climate change and livestock: impacts, adaptation, and mitigation. Clim Risk Manag 16:145–163

Segele ZT, Lamb PJ, Leslie LM (2009a) Large-scale atmospheric circulation and global sea surface temperature associations with horn of Africa June - September rainfall. Int J Climatol: A J Royal Meteorol Soc 29(8):10751100

Segele ZT, Lamb PJ, & Leslie LM (2009) Seasonal-to-interannual variability of ethiopia/horn of Africa Monsoon. Part I: associations of wavelet-filtered large-scale atmospheric circulation and global sea surface temperature. J Clim 22(12):3396–3421. https://doi.org/10.1175/2008jcli2859.1

Seiler RA, Hayes M, Bressan L (2002) Using the standardized precipitation index for flood risk monitoring. Int J Climatol: A J Royal Meteorol Soc 22(11):1365–1376

Seland Ø, Bentsen M, Olivié D, Toniazzo T, Gjermundsen A, Graff LS, Debernard JB, Gupta AK, He, Y-C, Kirkevåg A, Schwinger J, Tjiputra J, Aas KS, Bethke I, Fan Y, Griesfeller J, Grini A, Guo C, Ilicak M, … Schulz M (2020) Overview of the Norwegian earth system model (NorESM2) and key climate response of CMIP6 DECK, historical, and scenario simulations. Geosci Model Dev 13(12):6165–6200

Sere K (1996) Procedures and atomicity refinement. Inf Process Lett 60(2):67–74

Seré C, Steinfeld H, and Groenewold J (1996) World livestock production systems: current status, issues and trends

Sillmann J, Kharin VV, Zwiers FW, Zhang X, Bronaugh D (2013) Climate extremes indices in the CMIP5 multimodel ensemble: Part 2. Future climate projections. J Geophys Res: Atmos 118(6):2473–2493. https://doi.org/10.1002/jgrd.50188

Slingo J, Spencer H, Hoskins B, Berrisford P, Black E (2005) The meteorology of the Western Indian ocean, and the influence of the East African highlands. Phil Trans R Soc A: Math, Phys Eng Sci 363(1826):25–42

Steinfeld H, Wassenaar T, Jutzi S et al (2006) Livestock production systems in developing countries: status, drivers, trends. Rev Sci Tech 25(2):505–516

Stocker, Thomas F, Qin D, Plattner G-K, Tignor MMB, Allen SK, Boschung J, Nauels A, Xia Y, Bex V, and Midgley PM (2014) Climate change 2013: the physical science basis. contribution of working group i to the fifth assessment report of IPCC the intergovernmental panel on climate change.

Tan G, Ayugi B, Ngoma H, Ongoma V(2020) Projections of future meteorological drought events under representative concentration pathways (RCPs) of CMIP5 over Kenya, East Africa. Atmos Res 246(December):105112. https://doi.org/10.1016/j.atmosres.2020.105112

Tegegne G, Melesse AM, Alamirew T (2021) Projected changes in extreme precipitation indices from CORDEX simulations over Ethiopia, East Africa. Atmos Res 247:105156

Thornton PK (2010) Livestock production: recent trends, future prospects. Phil Trans R Soc B Biol Sci 365(1554):2853–2867

Thornton P, Nelson G, Mayberry D, Herrero M (2021) Increases in extreme heat stress in domesticated livestock species during the twenty-first century. Glob Change Biol 27(22):5762–5772

Vicente-Serrano SM, Beguería S, and López-Moreno JI (2010) A multiscalar drought index sensitive to global warming: the standardized precipitation evapotranspiration Index. J Clim 23(7):1696–1718

Volodin EM, Mortikov EV, Kostrykin SV, Galin VY, Lykossov VN, Gritsun AS, Diansky NA, Gusev AV, Iakovlev NG, Shestakova AA, Emelina SV (2018) Simulation of the modern climate using the INM-CM48 climate model. Russ J Numer Anal Math Model 33(6):367–374

Yukimoto S, Kawai H, Koshiro T, Oshima N, Yoshida K, Urakawa S, Tsujino H, Deushi M, Tanaka T, Hosaka M, Yabu S, Yoshimura H, Shindo E, Mizuta R, Obata A, Adachi Y, & Ishii M (2019) The meteorological research institute earth system model version 2.0, MRI-ESM2.0: description and basic evaluation of the physical component. 気象集誌. 第2輯 97(5):931–965.

Zeleke T, Giorgi F, Mengistu Tsidu G, Diro GT (2013) Spatial and temporal variability of summer rainfall over Ethiopia from observations and a regional climate model experiment. Theoret Appl Climatol 111(3–4):665–681

Zhou S, Park Williams A, Lintner BR, Berg AM, Zhang Y, Keenan TF, Cook BI, Hagemann S, Seneviratne SI, Gentine P (2021) Soil moistureatmosphere feedbacks mitigate declining water availability in Drylands. Nat Clim Chang 11(1):3844. https://doi.org/10.1038/s41558-020-00945-z